Investigating mixer-viscometer techniques for partially filled stirred tanks

Cunningham, Grace E.; Deshpande, Shreyasi; Simmons, Mark J.H.; O'sullivan, Jonathan

DOI:
10.1016/j.ces.2023.119340

Document Version
Publisher's PDF, also known as Version of record

Citation for published version (Harvard):
Cunningham, GE, Deshpande, S, Simmons, MJH & O'sullivan, J 2023, 'Investigating mixer-viscometer techniques for partially filled stirred tanks', *Chemical Engineering Science*, vol. 282, 119340. https://doi.org/10.1016/j.ces.2023.119340

Chemical Engineering Science 282 (2023) 119340

Contents lists available at ScienceDirect

Chemical Engineering Science

journal homepage: www.elsevier.com/locate/ces

Investigating mixer-viscometer techniques for partially filled stirred tanks

Grace E. Cunningham [a,b], Shreyasi Deshpande [b], Mark J.H. Simmons [a,*], Jonathan O'Sullivan [b]

[a] Centre for Formulation Engineering, School of Chemical Engineering, University of Birmingham, Edgbaston, Birmingham, B15 2TT, UK
[b] Unilever Research and Development, Port Sunlight Laboratory, Quarry Road East, Bebington, Wirral CH63 3JW, UK

ARTICLE INFO

Keywords:
Torque response
Close clearance agitators
Process parameters
Rheology
non-Newtonian fluids

ABSTRACT

Optimising the mixing stage of formulated product manufacture would help with resource utilisation, reducing cost, and developing superior products. However, accurately measuring and characterising mixing dynamics remains challenging. This study explores the use of traditional mixer-viscometer techniques, the Couette analogy and torque curve method, to infer viscosity from torque-speed data during batch mixing processes with partial fill levels (25 %, 62.5 %, 100 %) and varying fluid rheology. The methods yield comparable results in determining the mixer constant, *k'*, and consistency index, *K*, and flow index, *n*, at 100 % fill level but show limitations at lower fill levels due to non-linearity in torque-speed data. Changes in the torque-speed relationship were seen to occur around the point of vortex formation for lower fill levels ($Fr > 1$). Thus, these data points were excluded in the determination of *k'* for 25 % and *K* and *n* for 25 % and 62.5 %, but this didn't improve estimates for apparent viscosity and shear rate for any of the fluids or fill levels. To overcome these challenges, non-linear modelling techniques or data driven models may be required for inferring viscosity from torque at partial fill levels.

1. Introduction

The design and manufacture of formulated products is a major value-adding step, increasing the value of the constituent raw materials by up to two orders of magnitude. Furthermore, the estimated global market for formulated products is around €1.4 trillion (Sunkle et al., 2020; Smith, 2017). In efforts to make economic and environmental benefits, global manufacturers are driven to optimise resources such as raw materials and energy, where the manufacturing process plays a pivotal role.

The manufacture of formulated products typically involves a batch mixing stage, where raw materials are introduced to the vessel in a particular order and rate of addition, with controlled temperature profiles, mixing profiles, and other process conditions to attain optimal product structure. Mixing is a complex process which is not easily described, and many techniques have been developed to try and characterise mixing more meaningfully (Bowler et al., 2020). With Industry 4.0 gaining more relevance in manufacturing settings, companies are looking for cost-effective, simple measurement techniques that can be implemented on existing processes to enable process optimisation. Novel sensing technologies, whilst promising, often pose challenges due to expense and implementation barriers, particularly in industrial applications. An alternative approach involves using well-established sensors to monitor variables such as temperature, torque, pressure and flowrate, and implementing these into physical and data-driven models to infer difficult to measure variables, referred to as 'soft sensors' (Vieira et al., 2015). For example, Vieira *et al.* showed how temperature, flow rate and pressure sensor data can be inputted into a combination of physical models and artificial neural networks (ANNs) to model a spouted bed dryer to control the moisture content of milk powder during drying (Vieira et al., 2015).

The measurement of the torque on the agitator shaft is an ideal candidate for use in mixing process models (Bowler et al., 2020). For example, it enables the calculation of power per unit volume for use in scale-up, or in cases where a defined energy input is required to control product quality, power can be integrated with time (Xu et al., 2017; Altuna et al., 2016). Furthermore, in the laminar mixing regime, torque-speed data can also be used to infer viscosity. This is particularly beneficial in systems where the rheology is evolving during the manufacturing process and is related to the product structure (Bowler et al., 2020). However, there are limitations to the conditions where torque can be accurately measured, including sensitivity to changing environmental conditions which are inseparable from the manufacturing process, such as temperature, agitator speed, mixing regime, batch fill level and fluid rheology (Knight et al., 2001). Nevertheless, as one of the most economical and simple techniques, researchers have developed numerous ways to characterise mixing

* Corresponding author.
E-mail address: m.j.simmons@bham.ac.uk (M.J.H. Simmons).

https://doi.org/10.1016/j.ces.2023.119340
Received 27 June 2023; Received in revised form 24 August 2023; Accepted 25 September 2023
Available online 4 October 2023

systems and transform torque-speed data into viscosity-shear rate data, such as the power curve and torque curve method (Castell-Perez and Steffe, 1990), slope method (Rieger and Novak, 1973), and Couette analogy (Ait-Kadi et al., 2002).

The basis of all mixer-viscometry techniques is to characterise the mixer in terms of the mixer constant, k', which relates the impeller speed to the shear rate, and mixer coefficient, k'', which relates the torque to the viscosity - analogous to the shear rate constant and stress constant in rheometry. The characterisation of mixing systems can be simplified by developing correlations between dimensionless numbers. For Newtonian fluids in the laminar regime, the following relationship exists:

$$Po = K_P Re^{-1} \tag{1}$$

where, Po is the dimensionless Power number (-), Re is the dimensionless impeller Reynolds number (-), and K_P is the laminar power constant (-). Metzner and Otto expanded this relationship to non-Newtonian fluids by assuming the Newtonian viscosity term in the Reynolds number can be equated to the apparent non-Newtonian viscosity at a corresponding effective shear rate (Metzner and Otto, 1957). For example, for a power law fluid:

$$\mu = \eta = K\left(\dot{\gamma}_{av}\right)^{(n-1)} \tag{2}$$

where μ is the Newtonian viscosity (Pa s), η is the apparent non-Newtonian viscosity (Pa s) at the effective shear rate, $\dot{\gamma}_{av}$ (s^{-1}), K is the consistency index (Pa s^n), n is the flow index (-). The effective shear rate is related to the impeller speed by:

$$\dot{\gamma}_{av} = k' N \tag{3}$$

where N is the impeller speed and k' is the mixer constant, also known as the Metzner-Otto constant.

An alternative approach to the matching viscosity methods is the use of the Couette analogy (Ait-Kadi et al., 2002). The method equates the rheometer mixing geometry and vessel to a coaxial cylindrical bob rotating inside another cylinder (a Couette geometry), where the Couette analogue gives the same torque measurement as the agitator when at the same speed (Ait-Kadi et al., 2002).

Both the matching viscosity methods and the Couette analogy have been studied for various geometries and rheological properties. There is a lot of discussion in the literature about the effects of geometry, method, fluid rheology, and agitator speed on k'. The complexity of both the geometries utilised in mixer rheometry and the rheology of the fluids being measured leads to inconsistent conclusions. Despite the initial findings of Metzner and Otto suggesting k' might be independent of fluid rheology, it is now generally accepted that k' is dependent on the flow index of fluids when $n < 0.4$ (Bbosa et al., 2017; Brito de la Fuente et al., 1997; Mackey et al., 1987). However, there are conflicting opinions on how k' changes with flow index as it is difficult to decouple the effects from other rheological properties, *e.g.,* viscoelasticity and agitator speed (Castell-Perez and Steffe, 1990; Carreau et al., 1993).

Most attention has been focused on the effects of varying fluid rheology (Anne-Archard et al., 2006), geometry (impeller to cup ratios) (Brito de la Fuente et al., 1997), and rotational speed (Castell-Perez and Steffe, 1990); however little attention has been given to the effects of the fill level. Given that batch processes involve incremental ingredient additions, it would be useful to understand the effects of fill level on torque and viscosity. Sulaiman, *et al.* (Sulaiman et al., 2012) investigated the effect of fill level when using the torque curve method when the fill level was higher than the height of the agitator but didn't consider partial fill levels. They found that the mixer coefficient, k'', and mixer constant, k', had a power-law relationship as a function of fill height, and that a fill height equal to 1.5 times the height of the impeller gave the most accurate results for estimations of K and n. The study only investigated one type of paddle type agitator, with a small gap between the agitator and the vessel (d_i, impeller diameter/ D_c, cup diameter = 0.98).

In order to successfully implement online viscosity measurement into batch mixing processes with evolving fill level and rheology, it would be interesting to see if traditional mixer-viscometer techniques are suitable for partial fill levels and fluids with a range of rheological behaviours. Therefore, in this work, a rheometer with a helical ribbon mixing geometry has been used to collect torque-speed data at different speeds, batch fill levels, and for fluids with different rheology. Two different approaches to determine the viscosity from torque-speed data have been selected to determine if a particular method has better suitability for low fill levels. A range of fluids with various rheological properties have been selected, with the aim of covering the range of properties which might be seen during the manufacture of formulated products. This includes a range of consistency indexes and flow indexes, as well as some fluids which show viscoelasticity and possess a yield stress. Similarly, the fill levels have been varied from 25 % to 100 % to represent the range seen during a batch manufacturing process. The novelty of this work is the extension of typical mixer-viscometer techniques to partial batch fill levels and correlating the success of these methods to the unprocessed torque-speed data to determine the limits for these methods in practical applications. Hence, the objectives of this study are (1) to study the effect of process variables, namely fluid rheology and batch fill level on torque measurement, and (2) to determine how the mixer constant and mixer coefficient, and consistency index and flow index calculated using various mixer-viscometry techniques differ with the aforementioned variables. This will inform decisions on whether either of the methods investigated could be used in a practical application to infer viscosity from torque-speed data during a batch mixing process where the fill level is changing.

2. Materials and methods

2.1. Materials

Three non-Newtonian fluids with distinct rheological behaviours were studied: Carbopol® solution (CP), xanthan gum, glycerine and water solution (XG), and a lamellar gel network (LGN). Formulations and rheological properties are given in Table 1. The flow and consistency indices of the non-Newtonian fluids were determined by measuring the steady state apparent viscosity over a range of shear rates (10 – 500 s^{-1}) using a Couette or cross-hatched parallel plate geometry and fitting the data to the Ostwald-de Waele power-law model (4). See Table 2.

$$\tau = K\dot{\gamma}^n \quad and \quad \eta = K\dot{\gamma}^{n-1} \tag{4}$$

This is a simplification which can be satisfactorily applied in the shear rate range investigated, as the mixer-viscometer techniques which have been applied are most commonly based on power-law fluids. However, it does not account for the other complex rheological properties of the fluids and this will be considered in the discussion. LGNs over a larger shear range are more typically fitted to a Herschel-Bulkley model, where the fluid possesses a yield stress. The XG solution was also found to demonstrate viscoelastic behaviour which has not been accounted for in any calculations. Glycerine was the Newtonian fluid used for calibrating geometries (Palmera G995E; 99.5 % purity, supplied by KLK Oleo; viscosity 0.56 Pa s @ 30 °C; density 1260 kg m^{-3} @ 30 °C).

2.2. Experimental design

A Discovery Hybrid Rheometer III (TA Instruments, UK) was used to collect torque data over a range of tip speeds, *i.e.,* the tangential velocity of the impeller at its outermost point (0.125 m/s – 1.5 m/s). The rheometer was operated at each speed for 2 min, and an average of the data from the final minute was used in calculations to ensure the system had achieved steady state. Temperature was maintained at 30 °C. Three

Table 1
Formulations, consistency indices and flow indices of non-Newtonian fluids investigated.

Fluid	Formulation (w/w%)		Consistency index K (Pa s^n)	Flow behaviour index, n (-)	Density (kg m^{-3})
Carbopol® solution (CP)	Carbomer powder[a]	1.5 %	76.4	0.29	997
	Water	98.5 %			
Xanthan gum solution (XG)	Xanthan Gum[b]	5 %	36.6	0.25	1067
	Glycerine[c]	20 %			
	Water	75 %			
Lamellar gel network (LGN)	Cetearyl alcohol[d]	7.06 %	186.0	0.06	880
	Behentrimonium Chloride (BTAC)[e]	2.35 %			
	Water	90.59 %			

a) Carbopol® 980 polymer (supplied by Lubrizol), b) Xanthan gum (supplied by Jungbunzlauer (Basel, Swizterland)), c) Palmera G995E; 99.5% purity, supplied by KLK Oleo, d) cetyl alcohol (30 wt%) and stearyl alcohol (70 wt%), (Godrej Industries (India)), e) behentrimonium trimethyl ammonium chloride (BTAC), supplied by Clairant International Ltd. (Germany). This surfactant is provided at 70 wt% purity, where the remaining 30 wt% is comprised of dipropyl glycol, which acts as a processing aid.

Table 2
Dimensions of mixer rheometer geometries.

Mixer geometry dimensions	
Height, mm	36
Diameter, mm	31
Rheometer cup dimensions	
Height, mm	50
Diameter, mm	34
Other dimensions	
Gap between bottom of agitator and cup, mm	0.5

fluid fill levels were investigated (25 %, 62.5 %, 100 %). '100 % fill level' signifies the fill height of the fluid in the vessel is equal to the height of the impeller. The mixer geometry used is a 3D printed helical ribbon (HR) printed using direct metal laser sintering of titanium conducted by Laser Prototypes Europe Ltd (UK). The geometric considerations for the bespoke mixing element were based on representative examples found within mixing equipment. See Fig. 1.

As well as using a rheometer to measure torque, a transparent version of the vessel was set up to enable visualisation of the fluid (Fig. 2). A vessel of the same diameter as the rheometer cup was constructed from PVC and placed inside a PVC cube, filled with water, to prevent any distortion. An overhead mixer (Heidolph RZR 2021, Heidolph Instruments GmbH & Co. KG, Schwabach, Germany) was used to rotate the agitators over the total range of speeds. Video at 60 fps was collected for 5 s at each speed. Still images were randomly collected from the Video in post-processing.

2.3. Mixer-viscometer methods

2.3.1. Torque curve method

The torque curve method was developed by Mackey *et al.* to investigate the effects of different factors on the mixer constant, k' (Mackey et al., 1987). For example, Sulaiman *et al.* used this method to find k' and k'' as a function of fill height (Sulaiman et al., 2012). By substituting in the definitions of the Power number and Reynolds number, Eq. (1) can also be expressed as:

$$\frac{M}{d^5N^3\rho} = \frac{A\mu}{d^2N\rho} \tag{5}$$

where, M is torque (N m), μ is viscosity (Pa s), d is diameter of the impeller (m) and ρ is the fluid density (kg m^{-3}). Rearranging and simplifying gives an equation for viscosity as a function of torque, speed and a constant, k'', the mixer coefficient:

$$\mu = \frac{M}{Ad^3N} = \frac{k''M}{N} \tag{6}$$

By measuring torque-speed data for Newtonian fluids of known viscosity, k'' can be determined. To find the mixer constant, k', the apparent

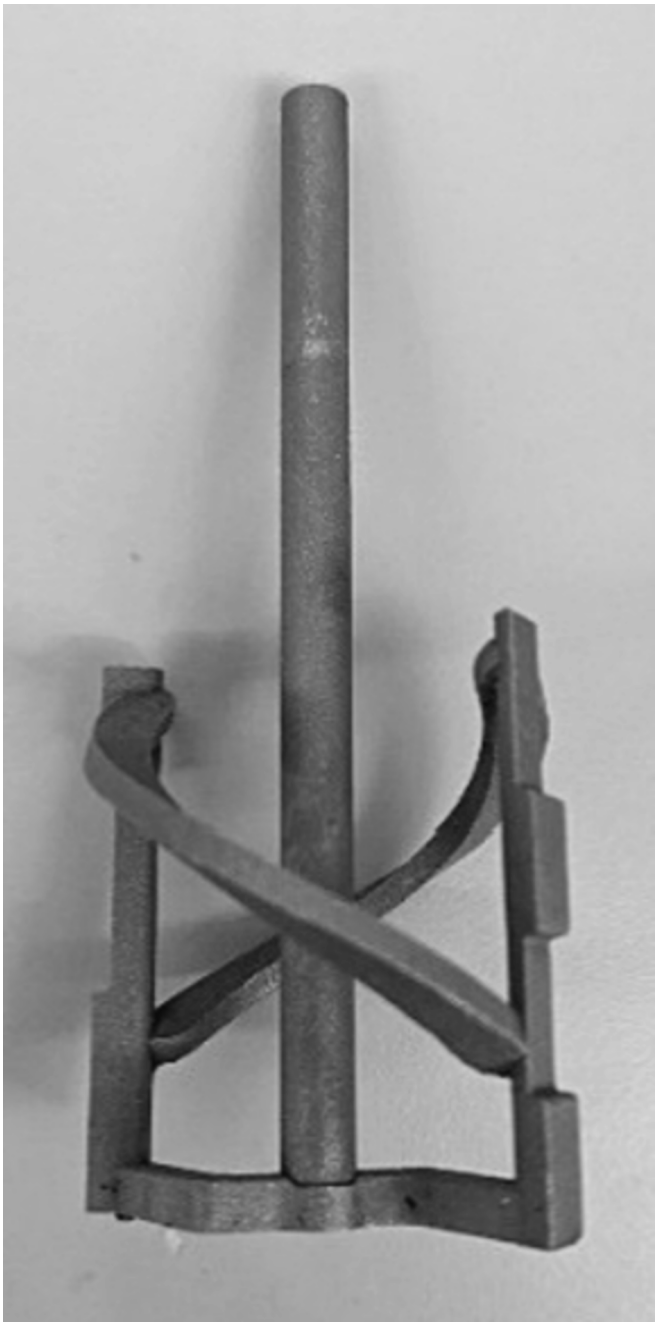

Fig. 1. 3D printed helical ribbon (HR).

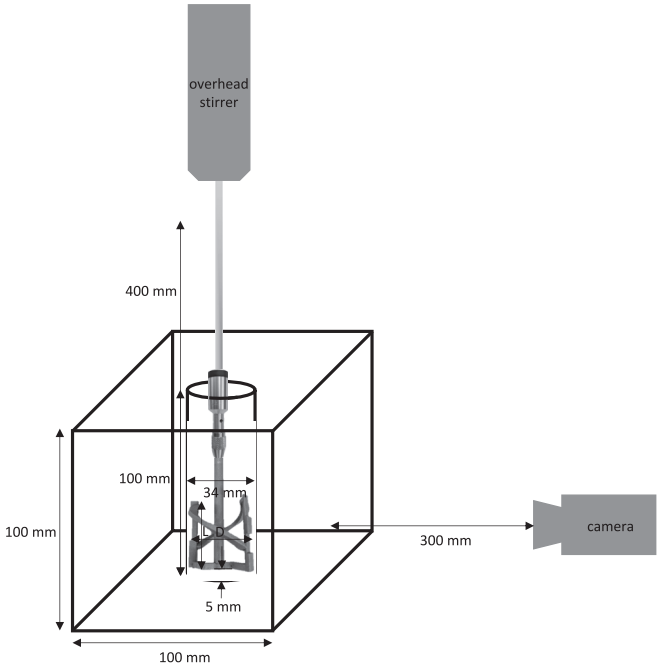

Fig. 2. Schematic of transparent version of rheometer set up with overhead stirrer, vessel and mixer geometry.

shear rate is determined at several speeds using a reference non-Newtonian fluid, typically a power-law fluid which has been characterised using conventional measuring techniques. $\dot{\gamma}_{av}$ is plotted against speed (*angular velocity, Ω, or N, rps)* and the gradient of the plot gives a value for *k'*. First, the matching viscosity assumption is applied:

$$\mu = \eta = K(\dot{\gamma}_{av})^{(n-1)} \tag{7}$$

Combining Eq. (5) and Eq. (6) gives an expression for the shear rate in terms of the mixer coefficient, torque, and speed:

$$\frac{k'' M}{\Omega} = K\left(\dot{\gamma}_{av}\right)^{(n-1)} \tag{8}$$

Rearranging Eq. (7), the average shear rate can thus be expressed as:

$$\dot{\gamma}_{av} = \left(\frac{k'' M}{\Omega K}\right)^{\frac{1}{n-1}} \tag{9}$$

Once *k'* and *k"* are determined, the apparent viscosity of new fluids can be determined from Eq. (6).

2.3.2. Couette analogy

An alternative approach to the matching viscosity methods is the use of the Couette analogy (Ait-Kadi et al., 2002). The method equates the rheometer mixing geometry and vessel to a coaxial cylindrical bob rotating inside another cylinder (a Couette geometry), where the Couette analogue gives the same torque measurement as the agitator when at the same speed (Choplin and Marchal, 2010). First, the equivalent Couette radius needs to be determined, using Eq.(10):

$$R_i = \frac{R_e}{\left(1 + \frac{4\pi N}{n}\left(\frac{2\pi\mu L R_e^2}{M}\right)^{1/n}\right)^{n/2}} \tag{10}$$

where, R_i is the equivalent Couette radius of the geometry (m), R_e is the radius of the vessel (m), and L is the length of the impeller (m). Ait-Kadi *et al.* found that the equivalent Couette radius was only slightly dependent on the flow index, *n*, thus it can be evaluated using a Newtonian fluid or well-characterised power law fluid (Ait-Kadi et al., 2002). The shear rate and shear stress vary in the gap between the geometry and the cup as a function of radius, *r*, and fluid rheology, namely the flow index, *n*. At a given radius, the shear rate is nearly independent of the flow index of the fluid – the optimal radius, *r**. For geometries where there is a small gap between the equivalent Couette radius, R_i, and the radius of the cup, R_e, ($R_i/R_e > 0.9$), the optimal radius can be taken as $r^* = R_i + R_e/2$. However, in cases where the gap is large, *r** must be found through graphical or analytical methods, *e.g.,* plotting calculated shear rate at different radii for various values of the flow index, *n* (Ait-Kadi et al., 2002); (Novontá et al., 2001). The radius at which the calculated shear rate values cross over, *i.e.,* are the same value for all flow indices is taken as *r** (Fig. 3). If the range of flow indices that must be covered is large, as in the case of this study, (n = 0.05 – 0.3), there may not be a single point at which the shear rates are equal for all flow indices. Some authors have used different radii for different ranges of flow indices *e.g.*, 0.05–0.1, 0.1–0.3 (Novontá et al., 2001). However, this is impractical in cases where the fluid rheology is not known. In this work, where there is not a single point, the cross-over value which was applicable over the largest range was used. The shear rate, $\dot{\gamma}_{av}$, and shear stress, τ (Pa), are then calculated from the below equations at the optimal radius, *r* (Eqs. (11) and (12)*. Apparent viscosity is determined from a plot of shear rate vs. shear stress.

$$\dot{\gamma}_{av} = \frac{\frac{4\pi}{n}\left(\frac{R_i}{r^*}\right)^{2/n}}{1 - \left(\frac{R_i}{R_e}\right)^{2/n}} N = k' N \tag{11}$$

$$\tau = \frac{M}{2\pi L r^{*2}} \tag{12}$$

2.4. Data analysis

Torque values were studied as a factor of fluid fill level and rheology. In order to determine the suitability of mixer-viscometer techniques at fill levels less than 100 %, two different methods were applied to convert torque-speed data to apparent viscosity – the torque curve method (TCM) (Mackey et al., 1987); (Castell-Perez and Steffe, 1990) and the Couette analogy (CA) (Ait-Kadi et al., 2002). For the TCM, the mixer constant, *k'*, has first been found using each non-Newtonian fluid as the reference fluid to determine the impact of rheology for the systems studied here. Then, the constants for the CP fluid have been used to calculate the apparent viscosity and average shear rate for each fluid, as CP showed the least deviation in *k'* between methods at 100 % fill level, and most closely follows the behaviour of power-law fluid. Plots of apparent viscosity versus average shear rate were used to determine the consistency and flow index (*K* and *n*). In the Couette analogy, the effects of fluid rheology on the equivalent Couette radius, R_i, optimal radius, *r**, and mixer constant, *k'*, were first investigated by using each fluid to determine the values, and then compared to the findings of Ait-Kadi

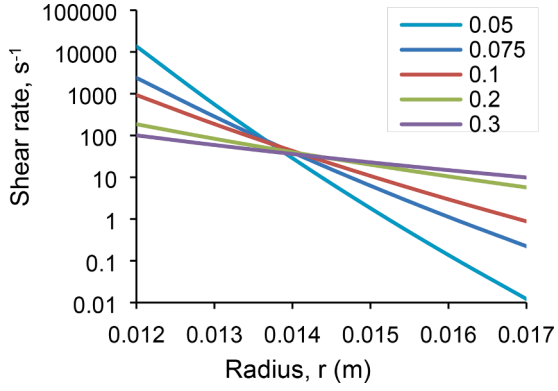

Fig. 3. Shear rate as a function of radius, r, and flow index, n (when Ω = 1 rad s^{-1}). Using R_i = 0.01326 m, calculated using CP as calibration fluid.

et al. for the 100 % fill level (Ait-Kadi et al., 2002). The values for the Newtonian fluid, glycerine, have been applied to find the apparent viscosity and shear rate for each fluid, and thus *K* and *n*.

3. Results and discussion

3.1. Effects of fill level on torque measurement

3.1.1. Newtonian fluid

The average torque values for the Newtonian fluid, glycerine, at different tip speeds are given in Fig. 4. Torque was measured across three fill levels: 25 %, 62.5 %, 100 %. A linear increase in torque with tip speed was observed at all fill levels ($R^2 = 0.99$), aligning with anticipated Newtonian fluid behaviour (Bbosa et al., 2017). Additionally, torque increased incrementally as a function of fill level, a trend congruent with results for granular high shear systems (Knight et al., 2001). Greater variability in measurements was seen at lower fill levels, attributed to the increased void in the vessel, allowing greater variability in the fluid-impeller contact. Whilst the variability also appears larger at higher speeds, the percentage deviation was proportionate across all speeds.

Fig. 5 shows the Power number calculated using the Newtonian torque data versus Reynolds number for all investigated fluid fill levels. The plots were fitted using regression to *Eq.* (1). to determine the power constant, *Kp*. For the range of speeds investigated, corresponding to a maximum Reynolds number of ~ 33, glycerine remains in the laminar mixing regime for all fill levels, which is typical for close clearance scrapers operating up to these Reynolds numbers (Brito de la Fuente et al., 1997). The laminar power constant, *Kp*, increases as a function of fill level, and is in the range of 104–208, which is in agreeance with literature values, which have been reported around 100–400 for close clearance scrapers at 100 % fill level (Jo et al., 2017); (Rudolph et al., 2009).

3.1.2. Non-newtonian fluids

Fig. 6 shows torque-speed plots for three non-Newtonian fluids across all investigated fill heights (25 %, 62.5 %, 100 %). The degree of linearity between torque and tip speed for non-Newtonian fluids is less than for the Newtonian fluid (Fig. 4).

Of the three non-Newtonian fluids, XG displayed behaviour most similar to the Newtonian fluid (Fig. 6a). However, a notable difference is that the torque does not intercept at zero. This trend was observed across all non-Newtonian fluids and is attributed to factors such as the fluids approaching a zero-shear viscosity plateau at very low shear rates or possessing a true yield stress. Thus even at low tip speeds a significant torque response is measured (Larsson and Duffy, 2013); (Cortada-Garcia et al., 2017). XG exhibits the lowest torque values of the non-Newtonian fluids, corresponding with its lowest consistency index, *K*. In general, the higher viscosity of the non-Newtonian fluids reduced torque variability at each speed compared to the Newtonian fluid (Fig. 4).

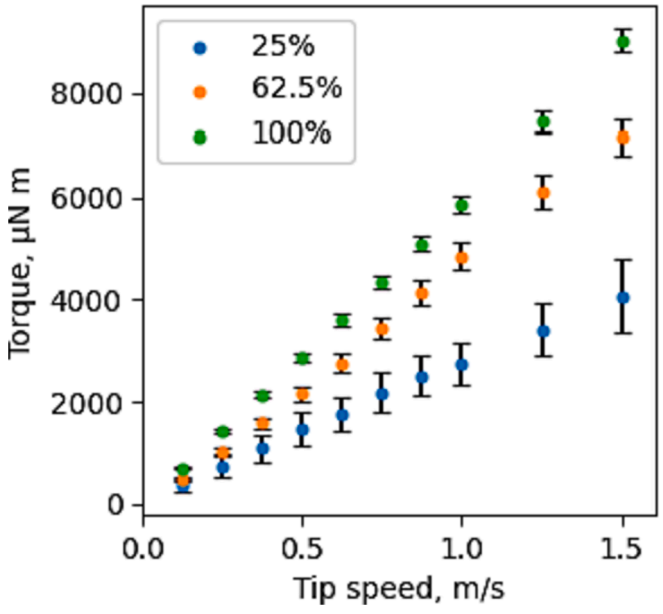

Fig. 4. Torque as a function of tip speed for glycerine at three fill levels (25%, 62.5%, 100%).

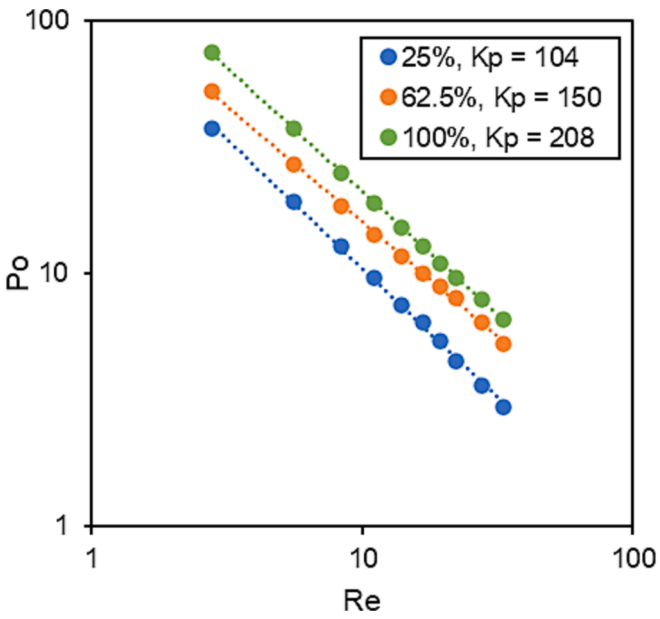

Fig. 5. Power curves for investigated fill levels, 25%, 62.5%, 100% determined using glycerine.

In the cases of CP and LGN, the torque response exhibited more variability as a function of tip speed and fill level. For CP at 100 % fill level (Fig. 6b), the torque response generally increases linearly with speed, whilst for LGN (Fig. 6c), a clear trend is absent. Torque initially increases to a maximum around 0.625 m/s, before decreasing and then slightly increasing again. The reduction in torque is attributed to air incorporation, reducing fluid density, whilst the subsequent rise potentially indicated a transition to turbulent or transitional regimes necessitating higher energy consumption due to increased radial and axial velocity flow components (Bbosa et al., 2017); (Rahimzadeh et al., 2022).

For CP at 62.5 % fill level, there is a large variation in the torque response recorded for the first three tip speeds, which could be related to the high viscosity of the fluid (Fig. 6b). It is likely that at lower tip speeds, not all of the fluid is engaged in flow, evidenced by visual inspection of the fluid in the vessel (Fig. 7) (Bbosa et al., 2017). For LGN at 62.5 %, again the torque does not follow the expected trend, and there is little change in torque with tip speed up until 0.5–0.625 m/s (Fig. 6c). Above this speed, there is a steep increase in torque as a function of tip speed.

Similarly, for both CP and LGN at 25 % fill level at lower tip speeds, the torque response remains steady up until 0.5–0.625 m/s, when torque starts to drastically increase with tip speed (Fig. 6b and c). Analysis of images collected in the transparent system showed that at lower tip speeds, the fluid is mostly gathered centrally in the centre of to the agitator. Above 0.5 m/s, the velocity of the agitator causes the fluid to be propelled off the agitator and to the walls of the geometry, so less fluid is in contact with the agitator, and more fluid is located in the gap between the impeller and the wall. This increases the resistance of the impeller to force, increasing the torque required to achieve a given speed (Fig. 7).

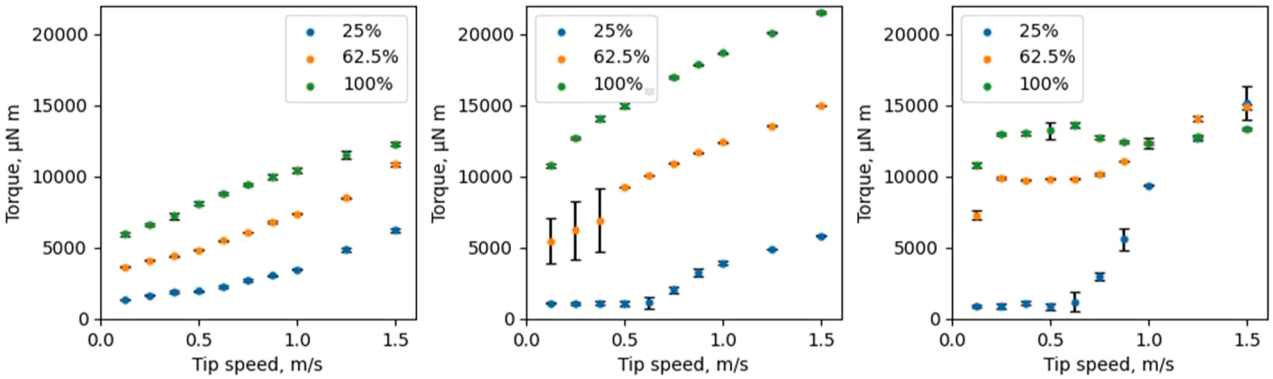

Fig. 6. Plots of torque vs tip speed for non-Newtonian fluid. From left to right, fluids: a) XG, b) CP, c) LGN.

(13)

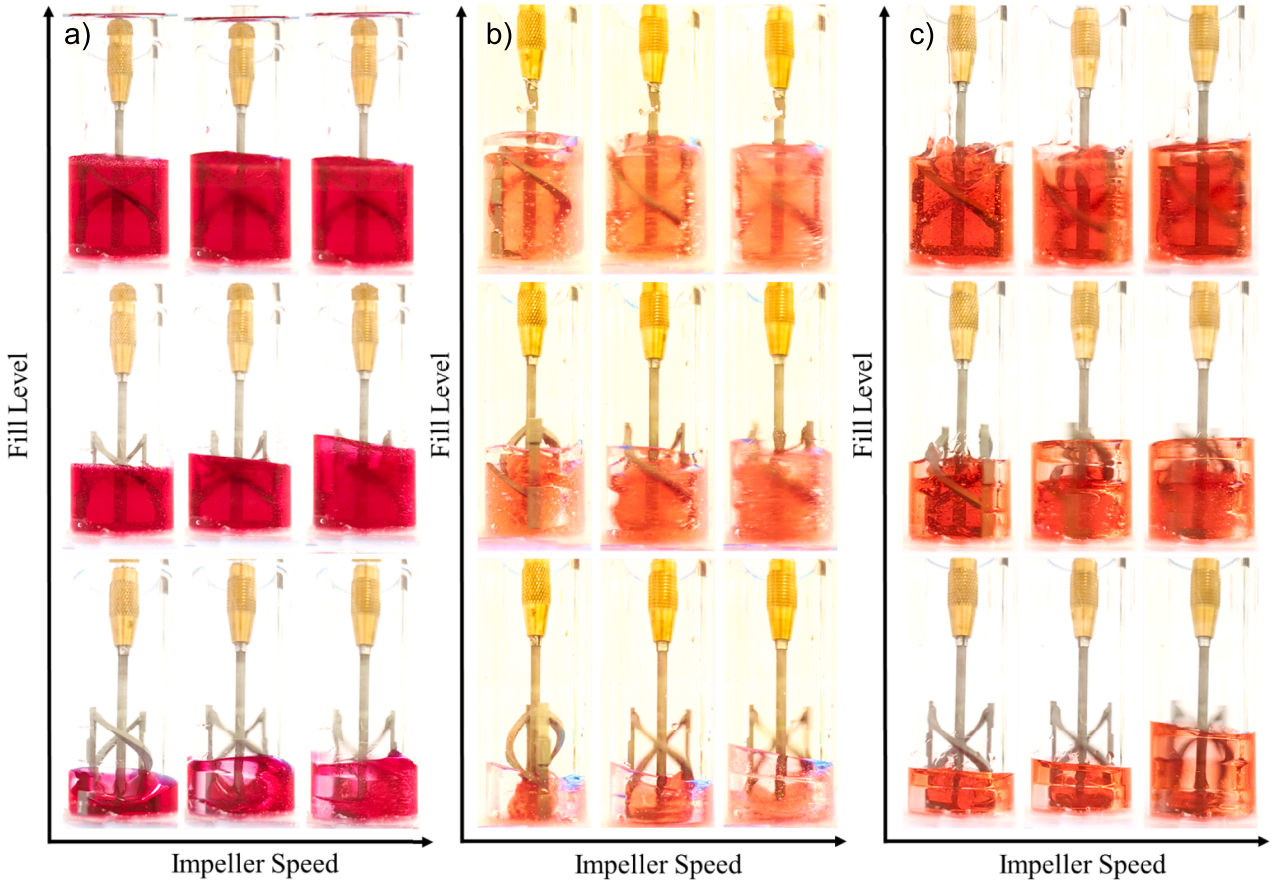

Fig. 7. Images from transparent set up showing a) GLY, b) XG and c) CP being mixed at 0.125 m/s (Fr = 0.05), 0.5 m/s (Fr = 0.82), 1 m/s (Fr = 1.8) at three fill levels, 25 %, 62.5 %, 100 % (LGN not included as non-transparent).

To attempt to quantify the point at which this transition from the 'bunched' flow regime to the 'centrifuged' state, the system was characterised by the Froude number. The Reynolds number was also considered to characterise the system but is difficult to determine at partial fill levels and requires knowledge of the apparent viscosity of the system. The Froude number was selected as it signifies the point at which vortex formation occurs. When Fr $<$ 1, flow is subcritical, and no vortex is present. At Fr $=$ 1, this signals the onset of vortex formation. When Fr $>$ 1, flow is supercritical, meaning that for a n unbaffled vessel, a vortex will form. The Froude number equation for a stirred tank is given in Eq. (13).

$$Fr = \frac{v^2}{gD} \tag{13}$$

where, Fr is the dimensionless Froude number, v is the velocity of the fluid (tip speed for stirred vessel), g is gravity, and D is the diameter of the impeller. The Froude number was calculated for each speed and was found to first be greater than unity at 0.625 m/s (Fr at 0.5 m/s = 0.82, Fr at 0.625 m/s = 1.13). Fig. 7 shows how the position of fluid in the vessel and the impeller-fluid contact changes with impeller speed, and

therefore Froude number, for GLY, XG and CP. The difference in behaviour between the Newtonian fluid and non-Newtonian fluids is most apparent at the lower fill levels. For the Newtonian fluid, the fluid does not bunch around the centre of the impeller and maintains contact with more of the impeller even at greater speeds. Whilst for XG and CP, there is a transition from bunched to centrifuged when Fr < 1, particularly at the lower fill levels. Using image analysis alone it is difficult to fully characterise the flow regimes. PIV or other flow visualisation techniques may be useful for further characterising the systems in the future. However, the purpose of this work is to determine the suitability of mixer-viscometer techniques to partial fill levels.

When considering the suitability of mixer-viscometer techniques, the Froude number was considered as a possible limitation for where the techniques can be appropriately applied.

3.2. Comparison of techniques at 100 % fill level

3.2.1. Effect of mixer-viscometry method and fluid rheology on mixer constant, k', at 100 % fill level

The first step in assessing the suitability of mixer-viscometer techniques for partially filled vessels was to determine the effects of fluid rheology on the value of k' at 100 % fill level. Other authors have previously investigated the impact of fluid rheology and mixer-viscometry method on k' at normal fill levels so a detailed analysis will not be provided here (Castell-Perez and Steffe, 1990); (Ait-Kadi et al., 2002); (Bbosa et al., 2017). However, previous work has shown that the effects are dependent on system geometry and rheology, so it is important to understand how k' varies for this system. k' was calculated using the two methods discussed: torque curve method (TCM), and Couette analogy (CA). Table 3 shows the mixer constant calculated using both methods.

It is not possible to calculate k'_{TCM} using only a Newtonian fluid, so no comparisons to k'_{CA} can be made for GLY. The largest difference in k' between the two methods was for XG, whilst the results for LGN and CP were in closer agreeance (CV = 25–30 %, respectively). Furthermore, for each respective method, the values calculated for CP and LGN were similar to each other (Table 3). XG did exhibit viscoelastic behaviour, which helps to explain the discrepancies in k' compared to the other fluids. There have been several attempts to determine the impact of elasticity on the torque measured for complex geometries such as helical ribbons, but a consensus has not been reached. Carreau *et al.,* and Collias and Prud'Homme found that elasticity increased the torque measurements (Carreau et al., 1993); (Collias and Prud'Homme, 1985), whilst Rieger and Novak and Ulbrecht and Carreau were incongruent (Rieger and Novak, 1974); (J. lbrecht and P. Carreau, , 1985). Ultimately, the effects of elasticity are dependent on the geometry, operating conditions and other fluid rheological behaviours (Carreau et al., 1993); (Jahangiri, 2008).

The values for k'_{TCM} determined using LGN and CP were closest to k'_{CA} determined using the Newtonian fluid. Considering all cases, there was greater variation in k' due to the method used than the calibration fluid used, which was also seen by Bbosa *et al.* (Bbosa et al., 2017). Castell-Perez and Steffe found for the TCM that in general, higher values of n, and lower values of K, gave higher values of k' (Castell-Perez and Steffe, 1990). XG and LGN followed this trend, it would be expected that CP had a k' value between XG and LGN. This said, it was difficult to decouple other rheological properties, and the regression analysis required for the TCM contributes to errors. Furthermore, their study was based on paddle agitators, and the geometry also impacts the observed trends in k'.

Overall, at 100 % fill level, both methods gave values for k' which were in agreement with literature values for similar geometries (Brito de la Fuente et al., 1997), with the values for k' calculated using CP and LGN being in good agreement but using XG showing discrepancies, likely due to its viscoelastic behaviour. Furthermore, the CA generally gave higher values for k' than the TCM, also seen by Bbosa *et al.* (Bbosa et al., 2017).

Table 3
Mixer constant calculated using CA and TCM using different calibration fluids.

Fluid	k'_{CA} (-)	k'_{TCM} (-)
GLY	3.90	–
XG	9.17	1.74
LGN	5.71	3.44
CP	5.79	3.13

3.2.2. Effect of mixer-viscometry method on determination of k and n

Using the methods described in section 2.3, the mixer constant, k', and mixer coefficient, k'', were applied to the torque-speed data to approximate the shear rate and apparent viscosity for each fluid. For CA, k' and k'' determined using the Newtonian fluid, GLY, were used. For TCM, where it is not possible to determine k' with a Newtonian fluid, the value determined using CP was used (Table 3). The consistency and flow index, K and n, respectively, are determined from fitting a plot of apparent viscosity as a function of shear rate to the Ostwald-de-Waele equation (Eq. (1). Therefore, the flow and consistency index can vary with the shear rate range over which they are (1) measured, and (2) fitted to the Ostwald-de-Waele power law model (Chhabra, 2010). Table 5 shows the consistency indices, K, and flow indices, n, calculated for the investigated fluids for each method. The data in Table 5 shows that both the CA and TCM are suitable for determining the apparent viscosity and shear rates of the range of fluids investigated here when the fill level is at 100 %. K and n are in good agreement to when measured using conventional geometries (cross-hatched parallel plates). Any discrepancies between the methods can be explained by the typical errors in measuring K and n using conventional methods (~5%) and in the methods themselves *e.g.,* due to regression fitting.

3.3. Torque curve method for fill levels less than 100 %

The suitability of the chosen mixer-viscometer methods for determining apparent viscosity and shear rate has been demonstrated at 100 % vessel fill level. Employing a single value of k' for each method allows the estimation of apparent viscosity across a range of rheological behaviours. The next step is extending these methods to partially filled vessels, *i.e.,* fill levels less than 100 %.

The mixer constant, k', was determined at each speed for each non-Newtonian fluid using Eq. (8). The results are presented in Fig. 8.

For 100 % fill level, a linear relationship between the calculated shear rate and speed existed, thus a single value of k' is applicable across all speeds (Table 4). Similarly for 62.5 % fill level, the relationship between calculated shear rate and speed is sufficiently linear to approximate a single value of k' (R^2 = 0.93–0.98) (Table 4).

However, at the lowest fill level, the plot of calculated shear rate versus speed shows significant deviations from linearity. Firstly, the calculated shear rates are orders of magnitude larger than for 62.5 % and 100 % fill levels. This can be attributed to the much lower torque values for this fill level. Up to a certain speed (~40.27 rad s^{-1}, equivalent to tip speed of 0.625 m s^{-1}), the shear rate displayed some linearity, beyond which it either reduced or plateaued. This trend correlated directly with the torque-speed data (Fig. 6). When the torque does not increase linearly with tip speed, corresponding to either a change in the mixing regime, incorporation of air into the system reducing the density, a change in the shape or position of the fluid in the vessel, or a change in the flow index of the fluid at higher tip speeds, then a single value of k' is not appropriate.

The Froude number was previously utilised to characterise the point at which the fluid transitioned from being mostly in contact with the agitator, to being centrifuged towards the walls (Fig. 6). This principle was extended when determining k' at 25 % fill level. When $Fr < 1$, *i.e.,* below 0.625 m s^{-1}, the torque response is sufficiently linear to

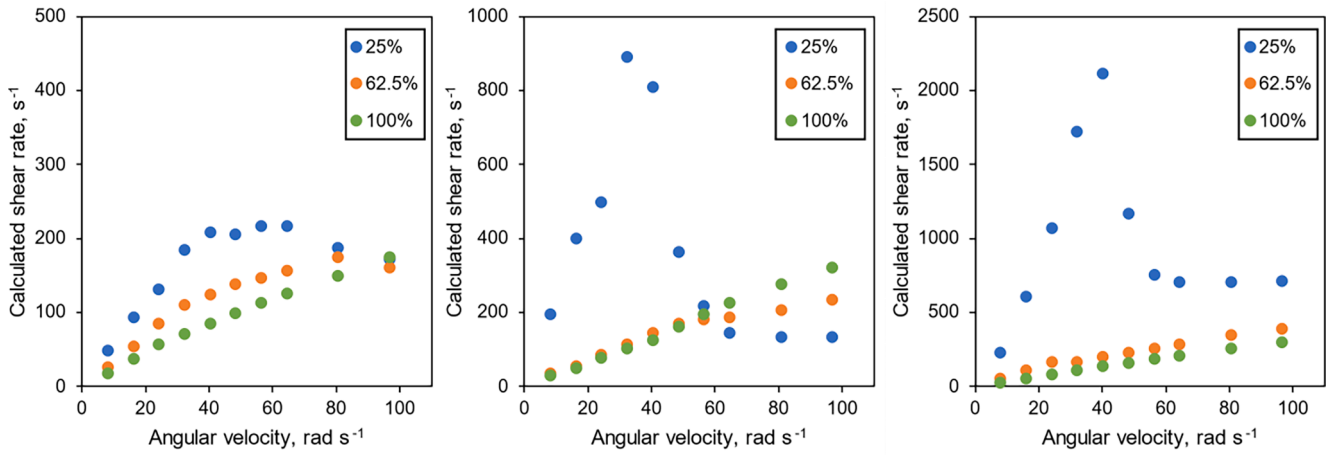

Fig. 8. Average shear rate calculated for each speed using the TCM for XG, LGN, and CP at three fill levels, 25%, 62.5%, 100%.

Table 4
Values determined for k' and k" using CA and TCM for all fill levels and using each fluid as the reference fluid.

Fluid	Fill Level	k' TCM	k" TCM	k' CA	k" CA
CP	25 %	61.4*	11,905	1.96	62,656
	62.5 %	3.62	7155	3.93	8497
	100 %	3.13	5945	5.79	3893
GLY	25 %	–	11,905	2.87	12,746
	62.5 %	–	7155	3.45	8072
	100 %	–	5945	3.9	6224
LGN	25 %	21.4*	11,905	1.28	48,800
	62.5 %	2.27	7155	7.67	3165
	100 %	3.44	5945	5.71	3537
XG	25 %	5.08*	11,905	3.92	11,991
	62.5 %	2.42	7155	5.35	4336
	100 %	1.74	5945	9.17	1930

*Determined using only first 5 data points/speeds (Fr < 1).

approximate a single value of k'. However, this still results in a value for k' orders of magnitude higher than that for 62.5 % and 100 % fill level (Table 4). In general across all fluids, there was not much difference in k'_{TCM} determined at 62.5 % and 100 %, but the method did not extend well to 25 % fill level, which gave considerably higher values for k', even when data was limited to a linear region. To note, the mixer coefficient, k'', is determined using Newtonian data, so is only a function of fill level and not fluid rheology.

Applying k'_{CP} across all fluids, the apparent viscosity and shear rate were estimated from the torque-speed data. At 100 % fill level, k'_{CP} gave the smallest deviation in K and n compared to conventional geometries. However, for lower fill levels there is the largest variation in k' as a function of fill height, especially for 25 % fill level. Fig. 9 shows plots of apparent viscosity as a function of shear rate calculated using TCM for the three non-Newtonian fluids at different fill levels. The dotted line represents the power law line fitted to the data measured using conventional geometry.

As previously discussed, at 100 % fill level, k'_{CP} effectively approximated the apparent viscosity and shear rate of the other fluids within acceptable error limits. At lower fill levels, applying a single value for the mixer constant and mixer coefficient (*i.e.,* for all speeds) data results in plots of apparent viscosity versus shear rate which reflect the shape of the torque-speed data (*cf.* Fig. 6). The apparent viscosity initially follows a power law relationship with shear rate, up until the point at which the torque deviates from linear behaviour (~0.625 m s^{-1}). This marks the transition to supercritical flow and vortex formation, *i.e.,* Fr > 1. Above

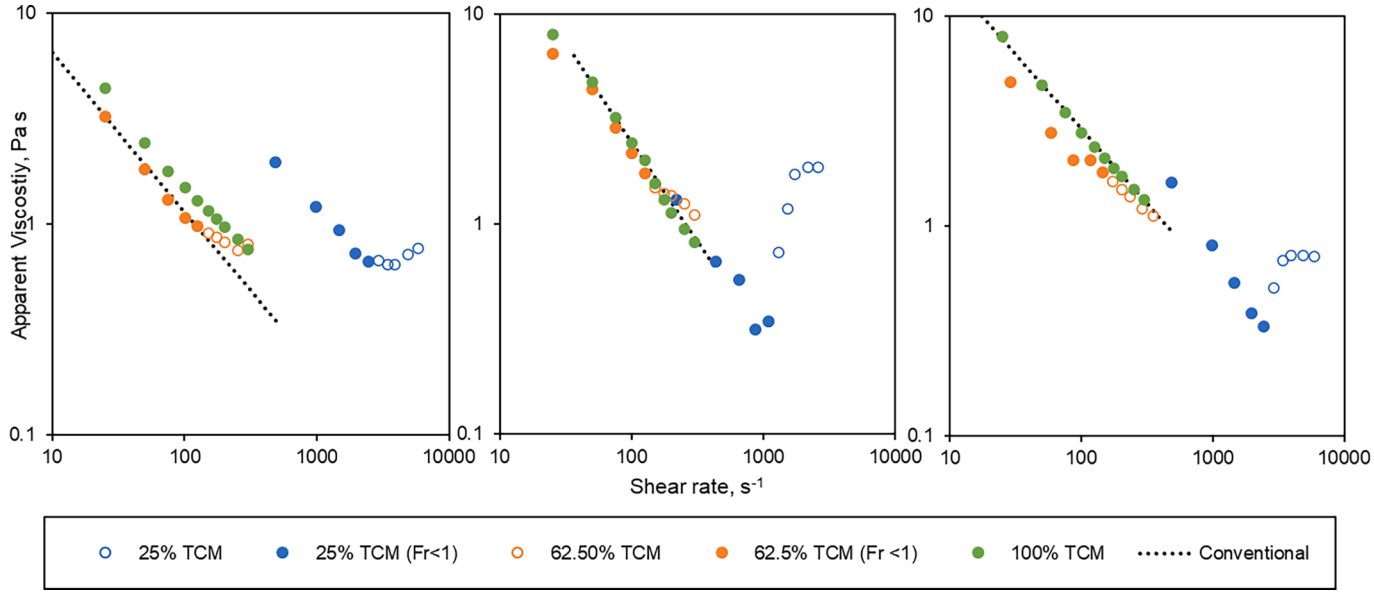

Fig. 9. Plots of apparent viscosity versus shear rate determined using TCM for a) XG, b) LGN, c) CP at 25%, 62.5%, 100% fill level.

this speed, the shape of the plot is related to the torque-speed data and follows a corresponding trend. For 25 % and 62.5 %, the flow and consistency indices (Table 5) were calculated using the full data, and data limited to Fr < 1.

For 62.5 % fill level, when the full data set is used, a power law model can be suitably fitted to the data, but the values for K and n are not in agreement with the conventional geometry. When the data is limited to $Fr < 1$, the estimates for K and n are somewhat improved, in particular the gradient of the slope is now closer to the conventional flow curve, and therefore the flow index is more representative of conventional geometry. For CP (Fig. 9c), the first three data points do not follow the same gradient as the rest of the data. Referring to the torque-speed data, this is where large variability was seen due to not all of the fluid being engaged in flow. This suggests that whilst the Froude number can be useful in determining the limits of where a single value of k' can be applied for each fill level, in fact the success of the technique is reliant on the general flow regime.

Similar results were seen for 25 % fill level, where the data initially follows a typical power law flow curve trend, up until shear rates equivalent to a speed of 0.625 m/s. Due to the higher value of k' calculated for 25 % fill level, the plot is also shifted to higher shear rates for each speed. Using the whole dataset, it was not possible to determine K and n accurately, a power law model did not fit the data well (R^2 = 0.3–0.86) and the values significantly differed from those measured with conventional geometry. Limiting the data to Fr < 1 again improved the fit of the power law model and gave values of n closer to the conventional geometry. However, due to the large value of k', the consistency index K determined was much larger using the TCM than the conventional geometry.

3.4. Couette analogy for fill levels less than 100 %

In the Couette analogy, the equivalent radius, R_i, is calculated using the torque Eq. (10). As the torque decreases with fill level, intuitively so does the equivalent radius and optimal radius, r^*. The shear rate and mixer constant, k', are calculated using (11. In general, k' increased as a function of fill level across all fluids and showed less variability at lower fill levels than when applying the TCM. This appears to be related to the interdependency of k' *and* k''. In the TCM, the mixer coefficient is predetermined using the torque measured for a Newtonian fluid and is assumed to be independent of the fluid rheology. However, for the Couette analogy, the mixer coefficient is retrospectively calculated from the calculated apparent viscosity, the non-Newtonian torque measurement and the optimal radius (Eq. (10) & (11). This results in k'' varying with fluid rheology and fill level, where the trends follow the same pattern as k' calculated in the torque curve method (Fig. 8), *i.e.,* for the lower fill levels for CP and LGN, the mixer coefficient is significantly higher (Table 4). So, whilst k' varies much less with fill level and rheology using the CA method, k'' is consequently influenced. The final difference between TCM and CA is that for CA, only a single value for k' can be determined for all speeds, so it is not possible to determine the effects of speed on k' for this method.

For the CA, k' determined using glycerine was applied to the other fluids and fill levels to approximate the apparent shear rate and viscosity from torque-speed data (Fig. 10). Similarly to the TCM, the method works well at 100 % fill level for all three fluids. At partial fill levels, similar results to the TCM were seen, where the apparent viscosity and shear rate follow a power law model up until the point where flow enters the supercritical regime. For all fluids, limiting the data gave closer approximations for K and n, and the plots of apparent shear rate as a function of viscosity are much closer to the conventionally measure flow curve. As there was less difference in k'_{TCM} and k'_{CA} at 62.5 %, there is less difference in K between the methods. However at 25 %, the differences in k' ($k'_{TCM} = 61.4$, $k'_{CA} = 3.9$) were evident in the different values for K. This was more evident when the data was limited to Fr < 1, and the power law model gave a better fit. Overall, the difference in K and n determined at 62.5 % fill level compared to using a conventional geometry is much greater than any differences which might be encountered through measurement error.

In conclusion, the application of the Froude number to assess data viability for mixer-viscometer methods isn't universally suitable across fluid rheologies. For instance, the case of CP at 62.5 % exhibited substantial torque variation for the first three data points, where the entire fluid wasn't engaged in flow, subsequently influencing apparent viscosity vs. shear rate plots. This underscores the need to comprehensively scrutinize torque-speed data and fluid flow, considering techniques like PIV or PEPT for improved insights into local flow velocities.

4. Conclusions

This study explored the impact of fill level, fluid rheology, and agitator speed on torque measurements. Subsequently, two mixer-viscometer methods—the Couette analogy and torque curve method—were employed to gauge their effect on k' calculation. Each method's ability to estimate apparent viscosity and shear rate using a single k' value at each fill level across the range of speeds was investigated. The primary objective was to assess whether typical mixer viscometer techniques could be employed in batch mixing scenarios, with evolving fill levels and fluid rheology, to develop a viscosity-based soft sensor from torque measurements.

In general, at 100 % fill level, CA and TCM gave similar values for k' when CP and LGN were used as the calibration fluids, but varied slightly more using XG, where CA gave much higher values. This was attributed to the viscoelastic nature of XG. When k'_{CP} was applied for the TCM, and k'_{GLY} for the CA, the resulting values for K and n were in reasonable agreement with those measured using conventional geometries.

At lower fill levels, challenges arose in calculating k' for certain instances, due to non-linear torque-speed data. An attempt to constrain data to Fr < 1, a rheology-independent metric, improved results, but high k' values persisted for 25 % fill levels in TCM, hindering the accurate prediction of shear rate and apparent viscosity. The observed vortex formation and torque changes were closely linked to fluid rheology attributes such as viscoelasticity or yield stress. Addressing this issue comprehensively for every fluid is impractical for potential online

Table 5
Consistency index, K, and flow index, n, determined for all fluid and fill levels using conventional measurement, by CA and TCM.

		Conventional		All Data Points				Data limited to Fr < 1			
Fluid	Fill Level	K	n	K_{CA}	K_{TCM}	n	R^2	K_{CA}	K_{TCM}	n	R^2
XG	25 %	36.6	0.25	7.89	20.19	0.59	0.86	25.54	164.49	0.29	0.99
	62.5 %			17.54	17.63	0.42	0.96	44.19	43.44	0.19	0.99
	100 %			33.88	38.08	0.31	0.99	–	–	–	–
LGN	25 %	186	0.04	0.38	0.1	0.70	0.3	51.19	245.30	0.03	0.99
	62.5 %			78.74	74.45	0.25	0.99	91.45	86.10	0.21	0.97
	100 %			203.31	189.36	0.05	0.99	–	–	–	–
CP	25 %	76.4	0.29	7.09	4.11	0.76	0.41	148.99	973.04	−0.03	0.99
	62.5 %			38.1	28.9	0.44	0.97	55.08	41.97	0.35	0.97
	100 %			90.65	79.48	0.28	0.99	–	–	–	–

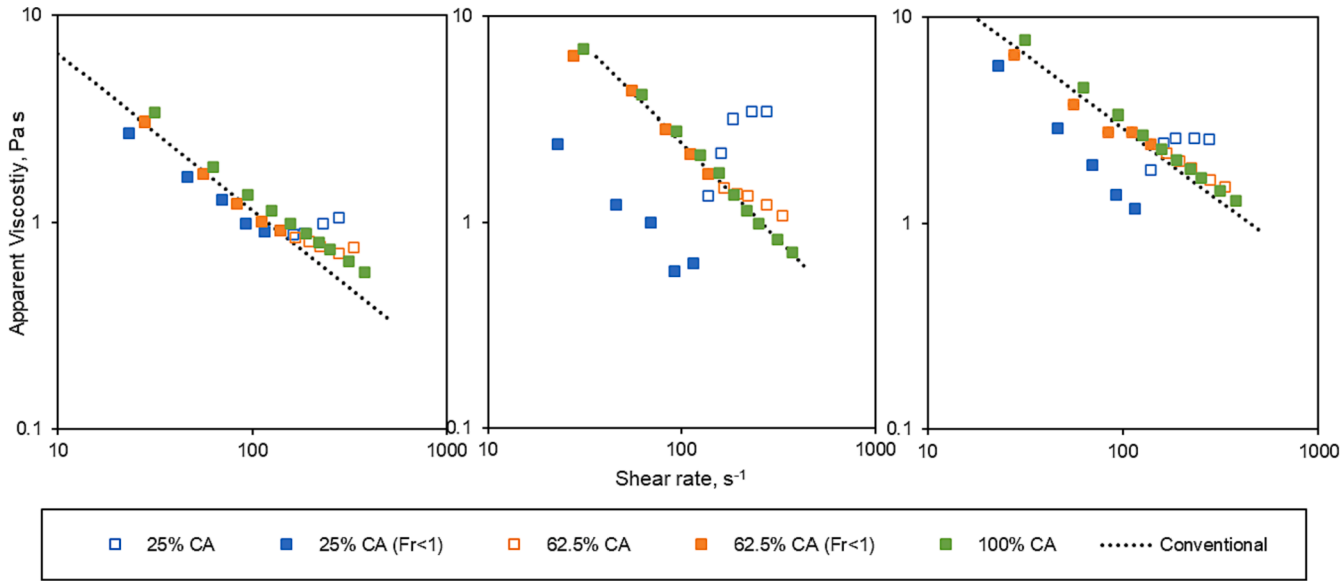

Fig. 10. Plots of apparent viscosity versus shear rate determined using CA for a) XG, b) LGN, c) CP at 25%, 62.5%, 100% fill level.

soft sensor applications. Further work could be done to provide approximation functions for the limitations of the mixer-viscometer techniques. This would require further data collection around the local fluid velocities and greater understanding of how the fluid-impeller contact changes as a function of fill height, fluid rheology and impeller speed.

In future studies, nonlinear modelling techniques or machine learning models like neural networks or random forest regression could prove more suitable for modelling viscosity from torque at partial fill levels. This research sets the stage for the incorporation of data-driven models in predicting apparent viscosity for partially filled vessels in larger-scale, industrial settings.

Declaration of Competing Interest

The authors declare that they have no known competing financial interests or personal relationships that could have appeared to influence the work reported in this paper.

Data availability

The data that has been used is confidential.

Acknowledgments

The authors wish to thank Unilever for their sponsorship and permission to publish this work. The authors would also like to acknowledge the financial support received from the Centre for Doctoral Training in Formulation Engineering (EPSRC grant no.EP/S023070.1).

References

Ait-Kadi, A., Marchal, P., Choplin, L., Chrissemant, A.-S., Bousmina, M., 2002. "Quantitative analysis of mixer-type rheometers using the couette analogy". Canadian J. Chem. Eng. 80.

Altuna, L., Romano, R.C., Pileggi, R.G., Ribotta, P.D., Tadini, C.C., 2016. Torque measurement in real time during mixing and kneading of bread dough with high content of resistant maize starch and enzymes. Int. J. Food Eng. 12 (8), 719–728.

Anne-Archard, D., Marouche, M., Boisson, H.-C., 2006. Hydrodynamics and Metzner-Otto correlation in stirred vessels for yield stress fluids. Chem. Eng. J. 125, 15–24.

Bbosa, B., DelleCase, E., Volk, M., Ozbayoglu, E., 2017. Development of a mixer-viscometer for studying rheological behavior of settling and non-settling slurries. J. Pet. Explor. Prod. Technol. 7, 511–520.

Bowler, A.L., Bakalis, S., Watson, N.J., 2020. A review of in-line and on-line measurement techniques to monitor industrial mixing processes. Chem. Eng. Res. Des. 153, 463–495.

Brito de la Fuente, E., Choplin, L., Tanguy, P., 1997. Mixing with helical ribbon impellers: effect of highly shear thinning behaviour and impeller geometry. Chem. Eng. Res. Des. 75 (1), 45–52.

Carreau, P., Chabra, R., Cheng, J., 1993. Effect of rheological properties on power consumption with helical ribbon agitators. Am. Inst. Chem. Eng. J. 39, 1421–1430.

Castell-Perez, M.E., Steffe, J.F., 1990. Evaluating shear rates for power law fluids in mixer viscometry. J. Texture Stud. 21, 439–453.

Chhabra, R., 2010. "Non-Newtonian Fluids: An Introduction", in Rheology of Complex Fluids. NY, Springer, New York.

Choplin, L., Marchal, P., 2010. Mixer-Type Rheometry. Rheology vol. 2.

Collias, D.J., Prud'Homme, R.K., 1985. The Effect of Fluid Elasticity on Power Consumption and Mixing Times in Stirred Tanks. Chem. Eng. Sci. 40 (8), 1495–1505.

Cortada-Garcia, M., Dore, V., Mazzei, L., Angeli, P., 2017. Experimental and CFD studies of power consumption in the agitation of highly viscous shear thinning fluids. Chem. Eng. Res. Des. 119, 171–182.

Jahangiri, M., 2008. Shear rates in mixing of viscoelastic fluids by helical ribbon impeller. Iran. Polym. J. 17 (11), 831–841.

Jo, H.J., Jang, H.K., Kim, Y.J., Hwang, W.R., 2017. Process viscometry in flows of non-Newtonian fluids using an anchor agitator. Korea-Australia Rheol. J. 29 (4), 317–323.

Knight, P., Seville, J., Wellm, A., Instone, T., 2001. Prediction of impeller torque in high shear powder mixers. Chem. Eng. Sci. 56 (15), 4457–4471.

Larsson, M., Duffy, J., 2013. An overview of measurement techniques for determination of yield stress. Annual Trans. Nordic Rheol. Soc. 21, 125–138.

lbrecht, J., Carreau, P., 1985. Mixing of viscous non-newtonian liquids. In: Mixing of Liquids by Mechanical Agitation. Gordon and Breach Science Publications, New York, New York, pp. 93–137.

Mackey, K., Morgan, R., Steffe, J., 1987. Effects of shear-thinning behaviour on mixer viscometry techniques. J. Texture Stud. 18, 231–240.

Metzner, A., Otto, R., 1957. Agitation of non-newtonian fluids. AIChE J. 3 (1).

Novontá, P., Landfeld, A., Kyhos, K., Houska, M., Strohalm, J., 2001. Use of helical ribbon mixer for measurement of rheological properties of fruit pulps. Czech J. Food Sci. 19, 148–153.

Rahimzadeh, A., Ein-Mozaffari, F., Lohi, A., 2022. Investigation of power consumption, torque fluctuation, and local gas hold-up in coaxial mixers containing a shear-thinning fluid: experimental and numerical approaches. Chem. Eng. Process. - Process Intesif. 177.

Rieger, F., Novak, V., 1973. Power consumption of agitators in highly viscous non-newtonian liquids. Trans. Inst. Chem. Eng. 51, 105–111.

Rieger, F., Novak, V., 1974. Power consumption for agitating viscoelastic liquids in the viscous regime. Trans. Inst. Chem. Eng. 52, 285–286.

L. Rudolph, V. Atiemo-Obeng, M. Schaefer and M. Kraume, "Power consumption and blend-time of co-axial tank mixing systems in non-Newtonian fluids," in *13th European Conference on Mixing*, London, 2009.

Smith, David. (2017) 'The Diversity and Synergies of Formulated Products', Centre for Process Innovation, 6th Feb. Available at: https://www.uk-cpi.com/blog/the-diversity-and-synergies-of-formulated-products (Accessed 3rd June 2023).

Sulaiman, R., Dolan, K.D., Steffe, J.F., 2012. Effect of fill level in mixer viscometry. J. Texture Stud. 43 (4), 319–325.

Sunkle, S., Saxena, K., Patil, A., Kulkarni, V., Jain, D., Chacko, R., Rai, B., 2020. Information extraction and graph representation for the design of formulated

products. In: Dustdar, S., Yu, E., Salinesi, C., Rieu, D., Pant, V. (Eds.), Lecture Notes Comput. Sci., vol. 12127. Springer, Cham.
Vieira, G.N.A., Freire, F.B., Freire, J.T., 2015. Control of the moisture content of milk powder produced in a spouted bed dryer using a grey-box inferential controller. Drying Technol. 33 (15–16), 1920–1928.
Xu, S., Hoshan, L., Jiang, R., Gupta, B., Brodean, E., O'Neill, J., Seamans, T.C., Bowers, J., Chen, H., 2017. A practical approach in bioreactor scale-up and process transfer using a combination of constant P/V and vvm as the criterion. Biotechnol. Process 33 (4), 1146–1159.